

# NUCLEAR MAGNETIC RESONANCE

Arnav Dutta,  
Lab Partner: Baran Altun  
(Dated: December 3, 2024)

## I. ABSTRACT

This experiment investigates the nuclear magnetic resonance (NMR) of hydrogen and fluorine nuclei in various samples to determine their respective g-factors. Through the use of a radio frequency coil and a static magnetic field, the resonance frequency was measured for water to find out the constant by which the current flowing through the coil is proportional to the magnetic field. Using the constant and the same technique, the resonance frequency was measured for hydrogen in glycerine and polystyrene, and fluorine in polytetrafluoroethylene (PTFE). Analysis of the resonance frequency as a function of magnetic field strength gave the g-factor values, for hydrogen, of glycerine ( $5.55 \pm 0.12$ ) and polystyrene ( $6.10 \pm 0.32$ ). The analysis of PTFE gave the g-factor, for fluorine, in PTFE ( $5.05 \pm 0.14$ ).

## II. INTRODUCTION

Nuclear Magnetic Resonance (NMR) is an analytical technique used in physics, chemistry and biology to investigate the magnetic properties of atomic nuclei since its discovery in the mid-20<sup>th</sup> century<sup>[1]</sup>.

This experiment aims to observe the Nuclear Magnetic Resonance of hydrogen and fluorine in liquids and solid samples. The resonance frequency and the corresponding magnetic fields will be analysed to determine the g-factor of the hydrogen in glycerine and polystyrene and the g-factor for the fluorine in polytetrafluoroethylene (PTFE). The g-factor is an impotent parameter as it provides insight into the magnetic moment and spin properties of atomic nuclei.

Another example of its application is Nuclear Magnetic Resonance Imaging (NMRI), a medical technique derived from NMR<sup>[3]</sup>. Through the use of the magnetic properties of hydrogen nuclei in the body to create detailed images of organs and tissues. Accurate g-factor measurements with a clear understanding of the NMR principles will lead to improved image quality and the creation of more specialized techniques, hence providing greater diagnostic precision.

The outcome of this report is to: demonstrate an enhanced understanding of NMR principles.

This experiment focused on hydrogen and fluorine nuclei due to their strong magnetic properties which will produce clear NMR signals as well as their abundant applications in pharmaceuticals, energy storage, chemical engineering, nanotechnology and materials science.

## III. THEORY

NMR is based on the magnetic properties of the nucleus, which in certain cases exhibit a spin.

Nuclear spin results when a nucleus has an odd number of protons, neutrons, or both. This leads to the nuclei having an intrinsic magnetic moment,  $\mu$ , and a spin angular moment,  $I_S$ . The relationship between  $\mu$  and  $I_S$  is:

$$\mu = -g\mu_n I_S \quad (1)$$

where  $\mu_n$  is the nuclear magneton ( $\mu_n = 5.051 \times 10^{-27} \text{ JT}^{-1}$ )<sup>[6]</sup> and  $g$  is the g-factor (dimensionless, magnetic moment).

The nuclear magnetic moment,  $\mu$ , can only orient in distinct directions with respect to an external static magnetic field,  $B_0$ . Each spin orientation corresponds to a perpendicular energy level given by:

$$E_k = -g\mu_n B_0 k \quad (2)$$

where  $k$  represents the spin quantum number ranging from  $-I_S$  to  $I_S$ .

When the sample is placed in a static magnetic field  $B_0$ , the nuclear spins are distributed over the energy levels according to the Boltzmann equation.

When the nuclei are exposed to a magnetic field ( $B_0$ ) of high frequency  $\nu$ , perpendicular to the static magnetic field  $B_0$ , the spins in the nuclei of the sample may be excited to jump between adjacent energy levels  $E_k$ . Therefore, the frequency  $\nu$  has to match exactly the energy spacing. This is resonance:

$$h\nu = \Delta E = E_k - E_{k+1} \quad (3)$$

$$E_k - E_{k+1} = -g\mu_n B_0(k) + g\mu_n B_0(k+1) \quad (4)$$

$$h\nu = \Delta E = g\mu_n B_0 \quad (5)$$

where  $h$  is Plank's constant ( $h = 6.626 \times 10^{-34} \text{ Js}$ )<sup>[5]</sup>.

## IV. METHOD

In this experiment, the NMR signals of hydrogen nuclei (Proton) and the fluorine nuclei were observed, both of which have a spin of  $I_S = \frac{1}{2}$  and two possible orientations with respect to the magnetic field ( $B_0$ ).

The sample was kept in a radio frequency (RF) coil, which was kept in the gap of a magnet, producing a homogenous field  $B_0$ , so that the spin transition between

the energy levels could be detected. Note that the static field is modulated at a constant frequency ( $\nu$ ) using modulation coils. Thus, the resonance signals were observed as a function of the magnetic field. Each time, the resonance condition (Eq.5) was met, the energy was absorbed from the RF coil due to the spin transition, with the NMR signal strength being proportional to the number of spins  $N$  in the sample.

Finally, the magnetic field, used later on for further calculation, was calculated using the proportionality:

$$B_0 = \alpha I_{CC} \quad (6)$$

where  $I_{CC}$  is the current through the 10 A coil.

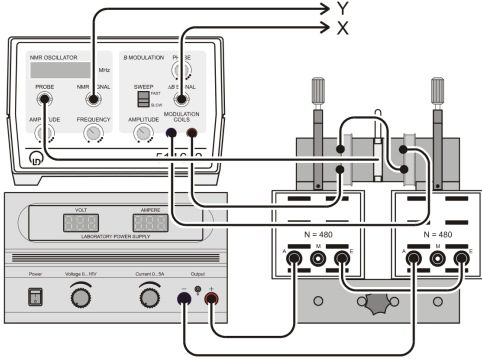


Figure 1. Electrical setup of the NMR experiment, schematically<sup>[4]</sup>

After the equipment was set up as shown in the equipment diagram (Fig. 1), the process of configuring, adding samples, observing changes and collecting data began.

First, ensure that the oscilloscope is set to XY mode. Then, adjust the NMR oscillator to fast sweep mode in the B modulation of the NMR oscillator. Next, tune the frequency to about 18.5 MHz (ensuring the red LED remains turned on and bright) by gradually increasing the HF (high frequency) amplitude. Finally, make sure that the source feeding is set to continuous current (CC) mode to maintain a fixed current regardless of the resistance of the coil. If the source cannot provide the desired current, it will automatically switch to continuous voltage, so it is important to fix this if it were to happen.

Shift the O-ring of the water sample tube so that the sample will be located approximately in the centre of the meeting chamber. Next, lower the sample into the measuring chamber, making sure it is oriented correctly. Note inserting the sample at an angle with too much force could damage the RF coil.

After the magnetic source set to continuous current, the frequency is varied between 17 MHz to 20 MHz for currents between 3 A and 4 A (few results went slightly over 4 A). Once the NMR signal was found, it was optimised by adjusting the HF amplitude and by making sure the signal was close to the centre of the screen (note perfect alignment was not always achieved

due to the high sensitivity of the oscilloscope). Then, adjust the phase of the signal until the signal of the up and down sweep coincide. Next, 4 readings of frequency were taken per reading of current.

## V. RESULTS

### A. Determining $\alpha$

The results of the investigation can be seen in the tables and figures below.

The uncertainty of  $I_{CC}$  was calculated to be half the resolution of the equipment used.

The Uncertainty of the average Frequency was calculated using the uncertainty of the average formula for small data sets:

$$\Delta \bar{\nu} = \frac{\nu_{\max} - \nu_{\min}}{2\sqrt{4}} \quad (7)$$

which gets simplified to:

$$\Delta \bar{\nu} = \frac{\nu_{\max} - \nu_{\min}}{4} \quad (8)$$

where  $\nu_{\max}$  is the largest value out of the 4 readings and  $\nu_{\min}$  is the smallest.

Using the results collected a graph was plotted to show the average resonance frequency as a function of current for water. Note the vertical error bars are the respective uncertainty in the average frequency. The horizontal error bars it the uncertainty of  $I_{CC}$ .

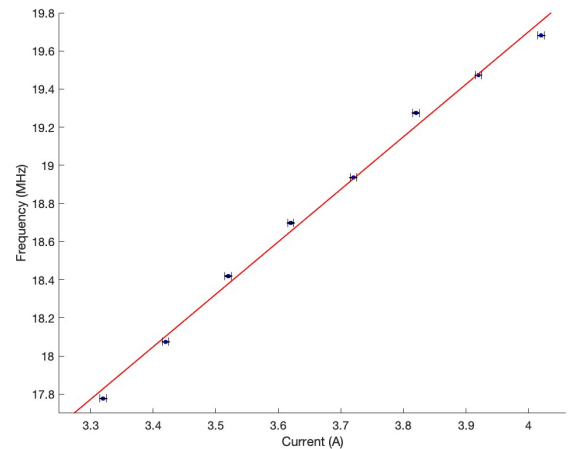


Figure 2. A graph of the average resonance frequency as a function of current for water

The gradient( $b_{\text{water}}$ ), uncertainty in the gradient ( $\Delta b_{\text{water}}$ ), y-intercept and the coefficient of determination( $R^2$ ) of the trend line in Fig. 2 was calculated using the LINEST function on Excel which performed the linear regression.

The gradient was calculated to have a value of  $(2.75 \pm 0.08) \times 10^6 \text{ s}^{-1} \text{ A}^{-1}$  with an  $R^2$  of 0.9945.

The first step for calculating  $\alpha$  was the following mathematical manipulation from combining Eq. 5 and Eq. 6 (note the g-factor in this equation was the g factor of hydrogen with a value of 5.5857:

$$h\nu = g\mu_n B_0 = g\mu_n(\alpha I_{CC}) \quad (9)$$

This simplified this to:

$$\nu = \frac{g\mu_n\alpha}{h} I_{CC} \quad (10)$$

which showed that the resonance frequency is a function of current.

Eq. 10 was then related to the equation of a straight line going through the origin ( $y = bx$ ), where the gradient of the line can be equated to:

$$b_{\text{water}} = \frac{g\mu_n\alpha}{h}$$

which is further manipulated to the equation used to work out the value of  $\alpha$ :

$$\alpha = \frac{hb_{\text{water}}}{g\mu_n} \quad (11)$$

The uncertainty of  $\alpha$  was calculated using the error prorogation formula for multiplication by a constant:

$$\Delta\alpha = \left| \frac{h}{g\mu_n} \right| \Delta b_{\text{water}} \quad (12)$$

With the use of Eq. 11 and Eq. 12  $\alpha$  was calculated to be  $(0.065 \pm 0.002) \text{ kg s}^{-2} \text{ A}^{-2}$ .

### B. Determining the Resonance Frequency as a Function of Magnetic Field Strength for Three Materials

The experimental producer was repeated (after collecting the data for water) for 3 more samples: glycerine, PTFE and poly-styrene.

A graph of resonance frequency as a function of magnetic field strength was plotted using the average resonance frequency collected and Eq. 6 where  $\alpha$ , calculated from the water sample, was substituted. This was repeated for the rest of the 3 samples.

The uncertainty of  $B_0$  ( $\Delta B_0$ ), which is used as the horizontal error bars in the graphs of resonance frequency against magnetic field strength, is calculated using the error propagation equation of multiplication:

$$\Delta B_0 = |B_0| \sqrt{\left( \frac{\Delta I_{CC}}{I_{CC}} \right)^2 + \left( \frac{\Delta \alpha}{\alpha} \right)^2} \quad (13)$$

where  $\Delta I_{CC}$  is 0.005 A.

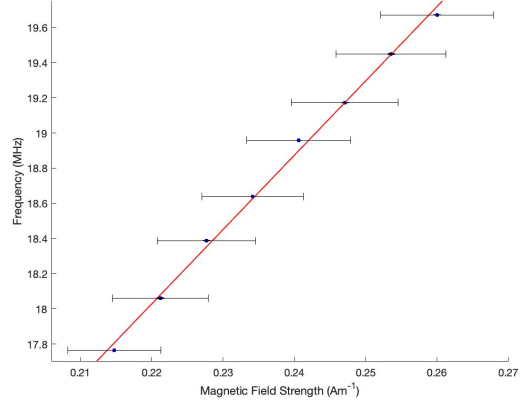


Figure 3. A graph of the average resonance frequency as a function of current for glycerine.

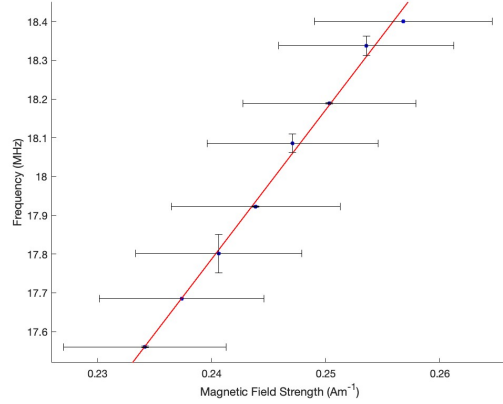


Figure 4. A graph of the average resonance frequency as a function of current for polystyrene.

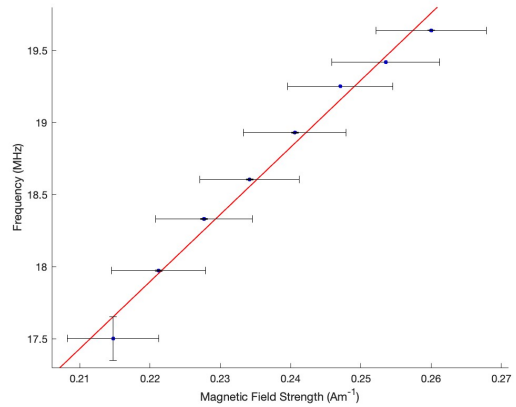


Figure 5. A graph of the average resonance frequency as a function of current for PTFE.

The vertical error bars were calculated using Eq. 8. The LINEST function was used again to work out the

gradient, its uncertainty, the y-intercept and the coefficient of determination for Fig.3, Fig.4 and Fig.5.

The gradient of the trend line in Fig.3 ( $b_{glyc}$ ) was calculated to be  $42.3 \times 10^6 \text{ A s kg}^{-1}$  with an uncertainty ( $\Delta b_{glyc}$ ) of  $0.9 \times 10^6 \text{ A s kg}^{-1}$  with a  $R^2$  of 0.9970.

The gradient of the trend line in Fig.4 ( $b_{PTFE}$ ) was calculated to be  $38.5 \times 10^6 \text{ A s kg}^{-1}$  with an uncertainty ( $\Delta b_{PTFE}$ ) of  $1.0 \times 10^6 \text{ A s kg}^{-1}$  with a  $R^2$  of 0.9956.

The gradient of the trend line in Fig.5 ( $b_{poly}$ ) was calculated to be  $46.5 \times 10^6 \text{ A s kg}^{-1}$  with an uncertainty ( $\Delta b_{poly}$ ) of  $2.4 \times 10^6 \text{ A s kg}^{-1}$  with a  $R^2$  of 0.9840.

### C. Determining g-factors of H and F

The first step in determining the g factor was to rearrange Eq.5 to make  $\nu$  the subject of the formula:

$$\nu = \frac{g \mu_n}{h} B_0 \quad (14)$$

Eq.14 showed that the resonance frequency ( $\nu$ ) is a function of magnetic field strength ( $B_0$ ), which can be related to the equation of a straight line ( $y = bx$ ). Using this relationship an equation involving the gradient of a  $\nu$  vs  $B_0$  graph and the g-factor was created:

$$b = \frac{g \mu_n}{h} \quad (15)$$

which can be rearranged to make the g-factor the subject of the formula:

$$g = \frac{b h}{\mu_n} \quad (16)$$

The uncertainty for the g-factor was calculated using the error propagation formula for multiplication by a constant:

$$\Delta g = \left| \frac{h}{\mu_n} \right| \Delta b \quad (17)$$

By substituting the gradients of the trend lines from the  $\nu$  against  $B_0$  graphs ( $b_{glyc}$ ,  $b_{PTFE}$ ,  $b_{poly}$ ) into Eq.16 and their corresponding uncertainties into Eq.17, we can calculate the g-factor for the hydrogen ( $g_H$ ) in glycerine and polystyrene, and the g-factor for the fluorine ( $g_F$ ) in PTFE.

The percentage difference (% Difference) was calculated using the following equation:

$$\% \text{ Difference} = \frac{|\text{Measured Value} - \text{Theoretical Value}|}{\text{Theoretical Value}} \times 100 \quad (18)$$

Sample:	Glycerine	Polystyrene
$g_H$	5.55	6.10
$\Delta g_H$	0.12	0.32
Percentage Difference (%)	0.72	9.26

TABLE I. A table showing all of the g factors for hydrogen values calculated from the observed data and their respective Uncertainty and Percentage difference

Sample:	PTFE
$g_F$	5.05
$\Delta g_F$	0.14
Percentage Difference (%)	3.84

TABLE II. A table showing all of the g factors for fluorine values calculated from the observed data and their respective Uncertainty and Percentage difference

## VI. DISCUSSION

The experiment results used were able to yield the g-factor for hydrogen and fluorine with resonance accuracy.

The calculated values for  $g_H$  in glycerine ( $5.55 \pm 0.12$ ) and polystyrene ( $6.10 \pm 0.32$ ) have a low percentage difference of 0.72% and 9.26%, respectively, when compared to the theoretical value ( $g_H = 5.5857$ )<sup>[7]</sup>. The calculated value of  $g_F$  in PTFE ( $5.05 \pm 0.14$ ) also had a low percentage difference of 3.84% when compared to its theoretical value ( $g_F = 5.2567$ )<sup>[4]</sup>. Thus showing the reliability of this experiment for calculating the g-factor for hydrogen and fluorine.

It should also be noted that systematic and random errors were observed in the experiment.

The systematic error observed was the presence of a non-zero y-intercept in all of the graphs plotted, implying that the trend line did not pass through the origin as it should have. The source of this systematic error could be the result of any unaccounted calibration offset in the instruments used or the influence of background magnetic fields. Another source of systematic error could be caused by the misalignment of the sample within the RF coil, creating a consistent variation. To avoid having these systematic errors in the future, the experiment should be repeated multiple times with different but identical sets of equipment. Here, the results will not be biased by specific apparatus and averaging the additional outcomes would reduce the impact of these systematic errors, provides more reliable and accurate results.

The random errors were seen when taking readings of the NMR oscillator due to the fluctuations, resulting in inconsistent frequency readings. This can be amended by the use of a data logger to log multiple frequency readings for short and fixed intervals to reduce the impact of the fluctuations. Another improvement would be to shield the setup to minimize external electromagnetic interference along with using a higher-quality magnet to create more uniform fields.

## VII. CONCLUSION

Despite the presence of errors in the experiment, the accuracy of the experiment is relatively high, which can be seen by the low uncertainty and high  $R^2$  values of the collected data. Proving that the experiment conducted provides a reliable g-factor for hydrogen and fluorine with resonance. Applying the refinements stated before will further increase the reliability and precision of the results and reduce their uncertainty.

Systematic errors present were due to equipment mis-calibration and alignment inconsistencies, and random

errors were due to frequency fluctuations. The errors were discussed and improvements were created. Overall, the accuracy of the experiment is relatively high and demonstrates that the experiment conducted provides a reliable g-factor for hydrogen and fluorine.

## VIII. ACKNOWLEDGEMENTS

I would like to thank my lab partner Baran Altun for his input and contribution to the measurements taken in this experiment. The equipment used was provided by the Department of Physics laboratory at King's College London.

## References

- 
- [1] Wikipedia contributors, *Nuclear magnetic resonance*, [https://en.wikipedia.org/wiki/Nuclear\\_magnetic\\_resonance#:~:text=Nuclear%20magnetic%20resonance%20\(NMR\)%20is,magnetic%20field%20at%20the%20nucleus](https://en.wikipedia.org/wiki/Nuclear_magnetic_resonance#:~:text=Nuclear%20magnetic%20resonance%20(NMR)%20is,magnetic%20field%20at%20the%20nucleus), Accessed: 2024-11-30.
  - [2] ScienceDirect, *Fluorine magnetic resonance imaging*, <https://www.sciencedirect.com/topics/medicine-and-dentistry/fluorine-magnetic-resonance-imaging>, Accessed: 2024-11-30.
  - [3] Wikipedia contributors, *Magnetic resonance imaging*, [https://en.wikipedia.org/wiki/Magnetic\\_resonance\\_imaging](https://en.wikipedia.org/wiki/Magnetic_resonance_imaging), Accessed: 2024-11-30.
  - [4] Indian Institute of Science, *Nuclear magnetic resonance (NMR)*, [https://physics.iisc.ac.in/~phylab/PH211\\_2019\\_3\\_NMR\\_LD.pdf](https://physics.iisc.ac.in/~phylab/PH211_2019_3_NMR_LD.pdf), Accessed: 2024-11-30.
  - [5] National Institute of Standards and Technology (NIST), *CODATA Value: Planck constant*, <https://physics.nist.gov/cgi-bin/cuu/Value?h>, Accessed: 2024-11-11.
  - [6] National Institute of Standards and Technology (NIST), *CODATA Value: nuclear magneton*, <https://physics.nist.gov/cgi-bin/cuu/Value?mun>, Accessed: 2024-11-11.
  - [7] 5CCP2100 Experimental Physics Laboratory Manual 2024/25, , Accessed: 2024-11-8.